



A Field Study to Investigate Moisture Loss from Early-Age Concrete Pavements

Jin-Hoon Jeong¹⁾ and Koil Choi²⁾

¹⁾ Pavement Research Group, Highway & Transportation Technology Institute, Korea Highway Corporation, Korea

²⁾ Construction Management Division, Construction Headquarters, Korea Highway Corporation, Korea

(Received May 10, 2004; Accepted August 30, 2004)

Abstract

A field test program was conducted for the newly placed concrete pavement of US Interstate Highway 10 between March 26th and 28th, 2003. The test section was located between Van Horn and Sierra Blanca in Hudspeth County approximately 130 km east of El Paso, Texas. The main objective of the test was collecting moisture-related data to validate the models of effective curing thickness, evaporation rate, and moisture-based maturity. Effect of moisture loss on drying shrinkage strain was studied using additional test instrumentation.

Keywords: concrete pavement, moisture, curing, drying shrinkage, temperature

1. Introduction

Available moisture in hardening concrete evolves into two types of water-one referred to as evaporable water held in both capillary and gel pores including interlayer pores and the other as non-evaporable water combined structurally in the hydration products.¹⁾ The sum of these portions equals the total water content in the paste. Water available in the capillary pores evaporates at the surface of concrete when it is exposed to ambient weather conditions. Because the predominance of moisture movement associated with evaporation occurs in the surface area, moisture variations within the cross-section of the concrete are found mostly near the surface.

Evaporation at the surface of a concrete slab can be defined as the net rate of vapor transport to the atmosphere.²⁾ This change in state requires an exchange of approximately 600 calories for each gram of water evaporated. Vaporization removes heat from water near the surface of the concrete slab being vaporized. Therefore, evaporation is another important factor to be considered in the analysis of thermally induced stresses and strains in a concrete slab in addition to conduction, convection, and radiation.³⁾

Evaporation is controlled by use of the appropriate curing method to minimize potential for undesirable cracking and deformation at early ages. The presence of water serves to enhance both hydration and strength development. As hydration advances and fills the space available in the capillary pores, capillary porosity continues to decrease and the amount of the gel pores increase. Gel pores tend to limit the movement of moisture through the capillary pores. Thus, the increase of hydrated product and reduced capillary porosity reduces the rate of evaporation. Drying shrinkage, due to evaporation, which leads to cracking or warping is also controlled by minimization of water loss from capillary pores.^{1, 4)} Models of effective curing thickness, evaporation rate, and moisture-based maturity were developed to provide indicator of curing effectiveness in the field. The main objective of the test was collecting moisture-related data to validate the models. The following briefly summarizes the test items.

- 1) Weather conditions (ambient temperature, ambient relative humidity, wind speed, and solar radiation)
- 2) Temperature and relative humidity of pavement (1.9, 7.6, and 17.8cm (0.75, 3, and 7inch) from surface)
- 3) Curing monitoring (relative humidity of ambient, surface, and concrete at 1.9cm (0.75inch) below pavement surface)
- 4) Relationship between drying shrinkage and concrete relative humidity (drying shrinkage test)

* Corresponding author

Tel.: +82-31-371-3368

E-mail address: j-jeong@freeway.co.kr

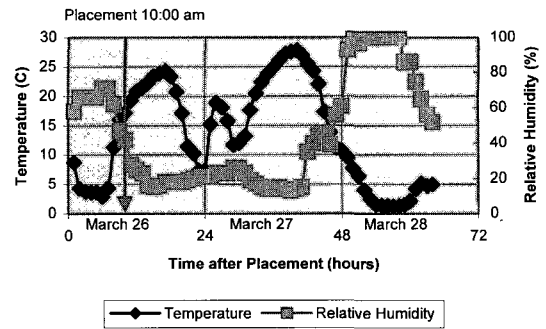
2. Construction and data category

A field test program was conducted for the newly placed concrete pavement of US Interstate Highway 10 between March 26th and 28th, 2003. The test section was located between Van Horn and Sierra Blanca in Hudspeth County approximately 130km east of El Paso, Texas. The continuously reinforced concrete pavement with 30.5cm (12inch) thickness was placed at 10:00am of March 26th on the existing 7.6cm (3inch) of asphalt pavement. During the period of data collection, a weather station was placed near the test section to measure hourly data of ambient temperature, ambient relative humidity, wind speed, and solar radiation. Curing monitoring system measured temperature and relative humidity of ambient, and surface and inside concrete. Temperature and relative humidity data of the pavement were also collected at 7.6 and 17.8cm (3 and 7inch) below top surface using chilled mirror sensors. Total strains of shrinkage bar specimens were measured using demac gauges to be correlated to their relative humidity by placing a chilled mirror sensor in another shrinkage bar specimen.

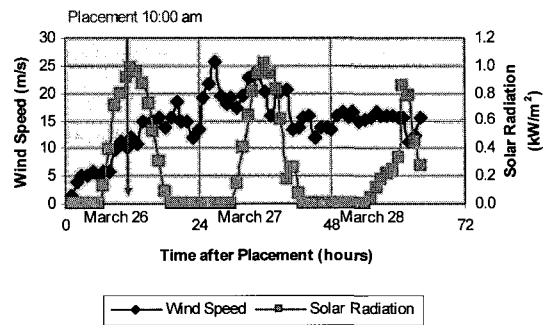
3. Weather conditions

A weather station was installed near the location where chilled mirror sensors and curing monitoring system were instrumented before the placement of the concrete. The weather station recorded ambient temperature, ambient relative humidity, wind speed, and solar radiation. It collected data at hourly intervals on a continuous basis. Radiation and convection play a dominant role in transferring heat between the slab surface and its immediate surroundings, while conduction plays a separate role in transferring heat within concrete slab. Maintaining higher levels of surface humidity is important for better curing quality, which can be achieved by high ambient relative humidity and low wind speed. Moisture variation or diffusion within the concrete slab is due to a difference in humidity between the slab surface and the concrete immediately below the surface.⁵⁾

Over the 3 days after placement of concrete, ambient temperatures ranged from a low almost 0 °C in the morning hours and to a high in the high 20's °C in the afternoon as shown in Fig. 1 (a). It is interesting to note that the unpredictable change in the daily pattern of ambient temperature. Significantly higher ambient temperature was observed in the morning of March 27th. Ambient relative humidity ranged from a low in the low 10% in the afternoon and to a high around 100% in the morning over the same period as shown in Fig. 1 (a). The daily pattern of ambient relative humidity also shows unpredictable changes.



(a) Ambient temperature and relative humidity



(b) Wind speed and solar radiation

Fig. 1 Weather conditions at Van Horn

Maximum relative humidity of 71, 26, and 100% were recorded in the morning of March 26th, 27th, and 28th, respectively. As shown in Fig. 1 (b), 1.01kW/m² of maximum solar radiation and 25.7m/s (57.5mph) of wind speed were recorded over the period. Maximum solar radiation was recorded between 12:00 and 1:00pm and was zero at night. Any daily pattern could not be found from the wind speed data while maximum wind speed was recorded at 3:00am of March 27th.

4. Temperature and moisture of pavement

Chilled mirror dew point and dry bulb temperature sensors were positioned in the pavement to measure moisture-related data at key locations. As shown in Fig. 2, two longitudinal bars (5th and 6th from a side of pavement) were cut before placement of concrete to place 1.3cm (0.5inch) thick PVC cylindrical wall. The PVC cylinder had both diameter and height of 30.5cm (12inch). The dew point sensors were protected from direct contact with the fresh concrete by use of brass casings, which are fixed into the PVC cylinder which was inserted within the pavement to ensure proper positioning of the sensors. The dew point sensors were located at 7.6 and 12.7cm (3 and 5inch) below the pavement surface.

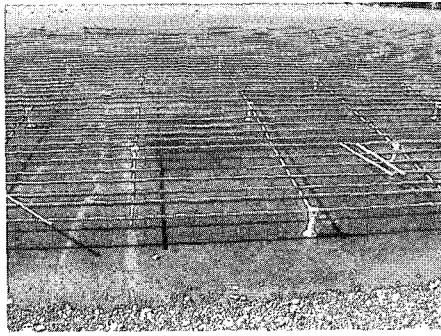
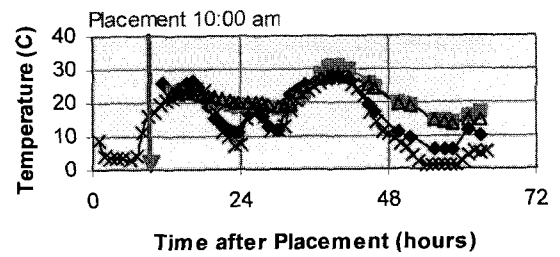


Fig. 2 Rebar cutting for instrumentation of chilled mirror sensors

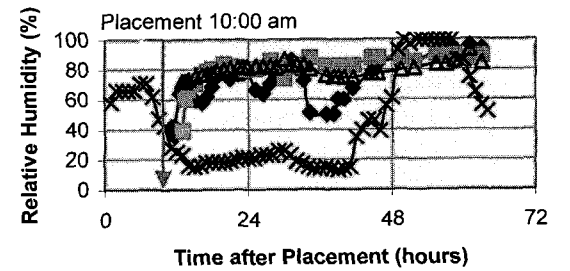
Several openings in the brass casings allowed the environment inside the casing to equilibrate with the environment inside the concrete. The sensors were sealed inside the casing to prevent contamination from ambient temperature and humidity conditions. Concrete temperature and relative humidity at 1.9cm (0.75inch) below pavement surface was measured by another dew point sensor of curing monitoring system which will be subsequently described in the next section.

Heat development due to hydration was reduced and retarded due to use of silica fume as a paving material and disadvantageous weather conditions such as low ambient temperature and high wind speed. Concrete temperature steadily decreased until next morning of construction at every depth of measurement due to low heat emission as shown in Fig. 3 (a). Because of the low heat development of concrete, daily maximum peaks of concrete temperature at every depth were almost same or a little bit higher than ambient temperature at those times. Concrete temperature measured at 1.9cm (0.75inch) below surface was more affected by ambient condition and, consequently, had closer values to ambient temperature than the temperature measured at 7.6 and 17.8cm (3 and 7inch). Concrete temperature measured at 7.6 and 17.8cm (3 and 7inch) had almost same values during the period of data collection.

Concrete relative humidity steadily increased until next morning of construction and then began to decrease because rate of evaporation and moisture diffusion of concrete significantly reduced at that time.⁶⁾ Relatively low concrete humidity was maintained at every depth of measurement during the period due to low ambient relative humidity as shown in Fig. 3 (b). However, concrete relative humidity increased again from the afternoon of that day because ambient relative humidity substantially increased to 100%. Concrete relative humidity measured at 1.9cm (0.75inch) below surface was more affected by ambient relative humidity as observed in concrete temperature trends.



(a) Temperature



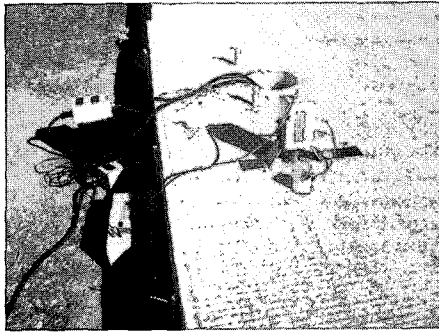
(b) Relative humidity

Fig. 3 Temperature and relative humidity at different depths of pavement

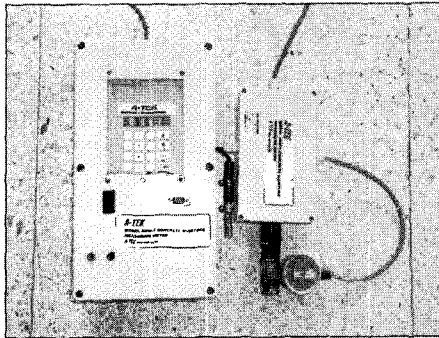
5. Curing condition and evaporation

As shown in Fig. 4 (a), a curing monitoring system manufactured by ATEK was installed immediately after placing concrete to collect data from the pavement when it cured. The ATEK system (Fig. 4 (b)) includes a plastic casing, as noted in Fig. 4 (c), connected to an aluminum stand that supports the weight of the curing monitoring system which is inserted approximately 5.1cm (2inch) into the concrete. There are four holes in the casing 1.9cm (0.75inch) below concrete surface to allow the vapor pressure of the concrete to equilibrate inside the casing. The relative humidity inside the concrete was determined from a chilled mirror type sensor, which measures the dry bulb and the dew point temperature from inside the plastic casing. The surface sensor measures the relative humidity from inside a PVC cylinder with an inside diameter and height of 6.4cm (2.5inch) and 5.1cm (2inch), respectively as shown in Fig. 4 (b). The cylinder was placed on the pavement surface in an area cleared of the curing membrane such that the sensor will register the relative humidity just below the curing membrane.

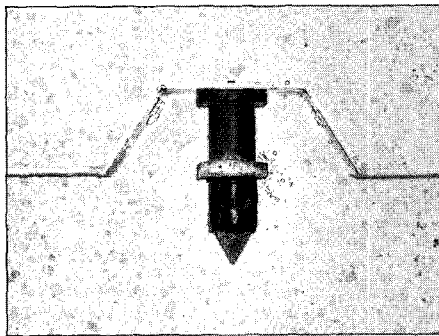
The third sensor measures the relative humidity just above the curing membrane.



(a) Instrumentation



(b) Sensors and reader



(c) Casing

Fig. 4 Curing monitoring system

The ambient relative humidity could not be measured because the sensor was out of order after a few hours of data collection. Although ambient relative humidity data collected from the weather station replace the ambient relative humidity of curing monitoring system, it does not seem to express actual moisture condition just above the curing membrane sufficiently. Relative humidity of both surface and inside concrete increased due to bleeding until next day of construction⁶⁾ and was higher than ambient relative humidity during the period as shown in Fig. 5. However, they decreased from next morning of construction due to reduced rate of evaporation and moisture diffusion as described previously.

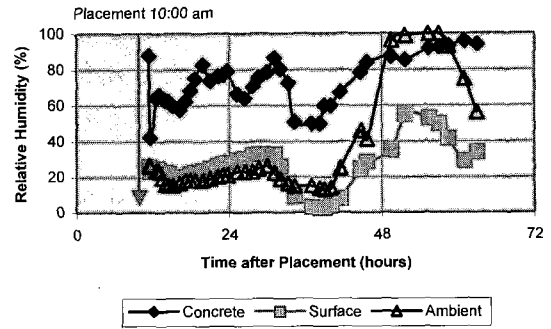


Fig. 5 Relative humidity of ambient, and surface and inside concrete

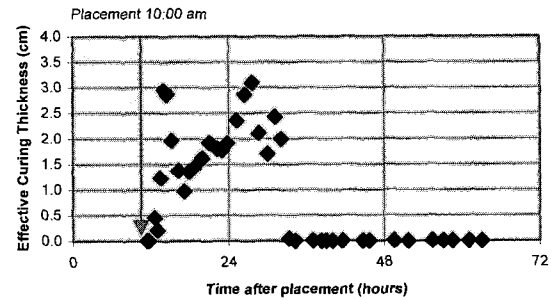


Fig. 6 Effective curing thickness of pavement with curing time

To quantify the curing effectiveness, the effective curing thickness concept originally introduced by Bazant and Najjar:⁷⁾

$$L = \frac{\ln \frac{H_s}{H_a}}{\frac{\partial H_s}{\partial x}}$$

where

- L = effective curing thickness (L)
- H_s = surface humidity, H_a = ambient humidity

was used. Effective curing thickness can be described as the equivalent layer of concrete that would provide the same degree of curing as the curing medium. Properly cured concrete has an effective curing thickness in the range of 7.6 to 12.7cm (3 to 5inch). In other words, the thicker the effective curing thickness is, the smaller the humidity variations near the surface.⁷⁾

The trend of effective curing thickness shown in Fig. 6 was similar to those of surface relative humidity because the effective curing thickness is governed mainly by the surface humidity.

The effective curing thickness increased throughout the duration of the bleeding when surface humidity also increased. Both effective curing thickness and surface humidity decreased simultaneously after bleeding. Calculated maximum value of effective curing thickness of 3.1 cm (1.2 inch) indicates poor curing condition was made due to severe weather conditions despite of curing compound application. Rate of evaporation was calculated using an evaporation model developed by Jeong and Zollinger.⁶⁾ Both net radiation and aerodynamic effects are considered in the model as:

$$E = \delta \frac{q_s''}{H_v} + J$$

where

- E = rate of evaporation from concrete due to both net radiation and aerodynamic effects (kg/m²/hr)
- δ = calibration factor for moisture condition of concrete surface
- q_s'' = solar radiation absorption through electromagnetic waves (kg/m/hr)
- H_v = heat of vaporization (heat removed from water on the surface of concrete slab being vaporized)
 $= 597.3 - 0.564T_s$ (cal/g)²⁾
 $= 427(597.3 - 0.564T_s)$ (m)
- J = rate of evaporation from concrete due to convective heat transfer, irradiation, and aerodynamic effects (kg/m²/hr)

The rates of evaporation computed from the model and test data were clearly affected by weather conditions. High wind speed and solar radiation, and low ambient relative humidity significantly increased the rate of evaporation as shown in Fig. 7. The rate of evaporation increased during bleeding and then decreased to zero.

6. Relation between moisture and shrinkage

Relative humidity of concrete has been recognized to have effect on the development of drying shrinkage.⁸⁾ However, the relationship between them has not been

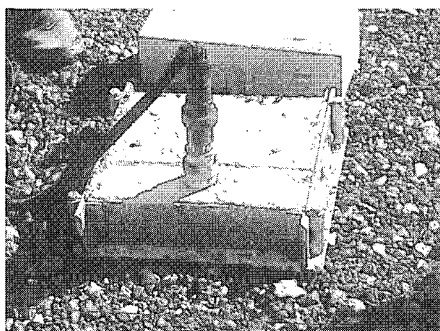


Fig. 8 Drying shrinkage test by ASTM C 157⁹⁾

studied sufficiently because of the troubles in accuracy of moisture measuring devices and instrumentation techniques. Three shrinkage bar specimens were made following the procedure of ASTM C 157.⁹⁾ Demac points were placed on the surfaces of two specimens and a chilled mirror sensor was inserted into another specimen by using a brass casing as shown in Fig. 8. Molds of the specimens were not demolded during the measurement period to prevent the drying of the specimens from their sides.

Because the chilled mirror sensor was installed at shallow depth (3.8cm (1.5inch)) and sides of the specimen could be effected by ambient, relative humidity was almost same as that measured at 1.9cm (0.75inch) from pavement surface as shown in Fig. 9(a). Drying shrinkage strains were calculated by subtracting calculated thermal strains from measured total strains as shown in Fig. 9(b). Thermal strains were calculated by multiplying temperature changes and 12 microstrains/^oC of coefficient of thermal expansion of the specimen which was approximately estimated by experimental experiences. The measurement continued in a laboratory of Texas Transportation Institute even after coming back from Van Horn. Linear relationship between drying shrinkage and relative humidity of the specimen was observed as shown in Fig. 9(c). It is the same trend observed in another laboratory test previously conducted (Fig. 10). Constant curing temperature and relative humidity of 50°C and 10% were maintained in the test.

7. Moisture-based maturity

Concrete hardens with increase of hydration products made by reaction between water and cement. The concrete should be nearly saturated by preventing evaporation from the surface to continue the hydration. Powers¹⁰⁾ suggested that hydration completely stopped when the relative humidity of the concrete decreased to 80%. Because the strength of concrete is significantly influenced by moisture level within the concrete and the moisture level is different with pavement depth (Fig. 11), existing maturity concepts was

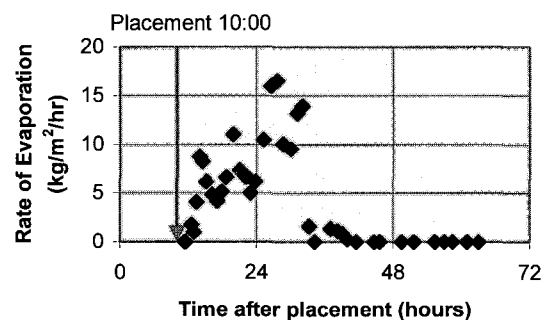
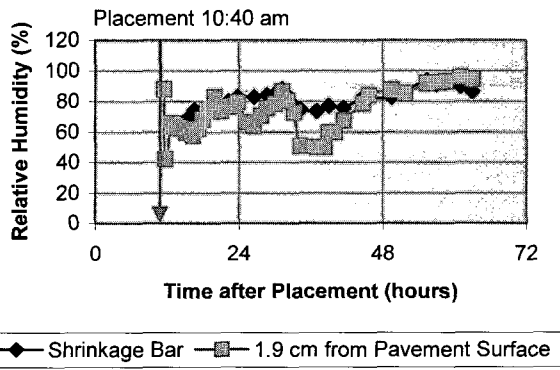
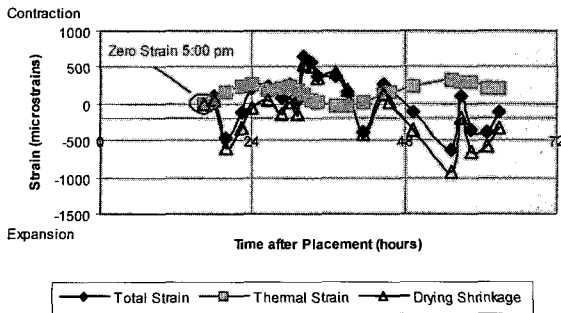


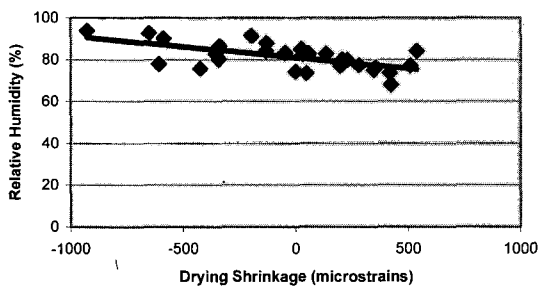
Fig. 7 Calculated rate of evaporation with curing time



(a) Relative humidity with curing time



(b) Drying shrinkage strains with curing time



(c) Drying shrinkage with relative humidity

Fig. 9 Relationship between drying shrinkage strains and relative humidity

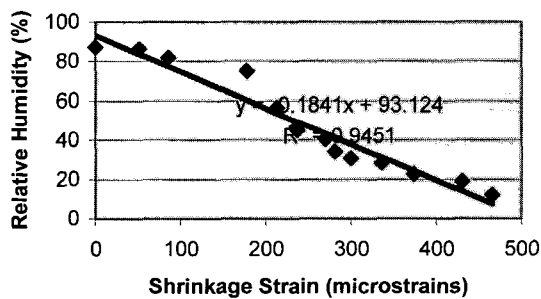


Fig. 10 Another test result of drying shrinkage strains with relative humidity

modified by including a moisture parameter in the maturity model:¹¹⁾

$$M'_H = \beta'_H \cdot \sum_0^t (T - T_0) \cdot \Delta t = \frac{\sum_0^t (T - T_0) \cdot \Delta t}{1 + (5 - 5H)}$$

where

- M'_H = moisture-based maturity
- β'_H = modified moisture parameter
- T = pavement temperature
- T_0 = reference temperature (= -10 °C)
- Δt = time interval
- H = pavement humidity

Moisture-based maturity was calculated on the basis of the temperature and moisture data as shown in Fig. 12. Relatively higher moisture-based maturity was calculated when relative humidity of pavement was high on the 3rd day after placement while lower moisture-based maturity was calculated during the period of low concrete relative humidity measurement.

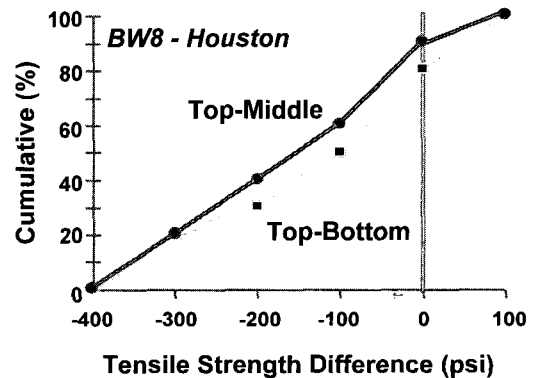


Fig. 11 Strength differences between different depths of pavement (Houston Test Section, 1psi = 6.895kPa)

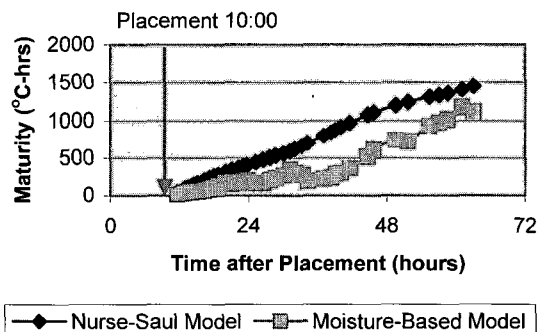


Fig. 12 Moisture-based maturity with curing time

8. Conclusions

Field measurements were made for the continuously reinforced concrete pavement to see environmental effects on the pavement. During the period of measurement, severe weather conditions such as high wind speed, rapid and large variations in ambient temperature and relative humidity influenced on the pavement, especially at shallower depths. Because heat development by hydration was restrained due to the weather condition and material property of concrete, pavement temperature was not increased so much. Relatively low initial effective curing thickness and high rate of evaporation were calculated due to poor curing conditions caused by the severe weather. The evaporation model may need to be calibrated for the high wind speed because lower levels of wind speeds were used as a parameter to develop the model. Linear relationship between drying shrinkage and relative humidity of concrete was observed by drying shrinkage test. Although reasonable trend of moisture-based maturity was calculated using collected temperature and moisture data, a cumulative moisture parameter which utilizes moisture history of concrete needs to be developed to consider the moisture variation due to environmental conditions in field.

References

1. Mindess, S. and Young, J. F., "Concrete," Prentice-Hall, Inc., Englewood Cliffs, NJ, 1981.
2. Linsley, R. K., Kohler, M. A., and Paulhus, J. L., "Hydrology for Engineers," 2nd Ed., McGraw-Hill, New York, NY, 1975.
3. Kapila, D., Falkowsky, J., and Plawsky, J. L., "Thermal Effects during the Curing of Concrete Pavements." *ACI Materials Journal*, Vol.94, No.2, 1997, pp.119~128.
4. Neville, A. M., "Properties of Concrete," 4th Ed., John Wiley & Sons, Inc., New York, NY, 1996.
5. Jeong, J. H., Wang, L., and Zollinger, D. G., "A Temperature and Moisture Module for Hydrating Portland Cement Concrete Pavements." *Proceedings, 7th Int. Conf. on Concrete Pavements*, Vol.1, Orlando, FL, 2001, pp.9~22.
6. Jeong, J. H. and Zollinger, D. G., "Development of Test Methodology and Model for Evaluation of Curing Effectiveness in Concrete Pavement Construction," *Transportation Research Record 1861*, TRB, National Research Council, Washington, DC, 2003, pp.17~25.
7. Bazant, Z. P. and Najjar, L. J., "Nonlinear Water Diffusion in Nonsaturated Concrete," *Materials and Structures*, RILEM, Vol.5, No.25, 1972, pp.3~20.
8. Bazant, Z. P. and Panula, L., "Practical Prediction of Time-dependent Deformations of Concrete. Part 1: Shrinkage, Part 2: Creep," *Materials and Construction*, Vol.2, No.65, 1978, pp.301~328.
9. ASTM, "ASTM C 157: Standard Test Method for Length Change of Hardened Hydraulic-Cement Mortar and Concrete," *Annual Book of ASTM Standards*, American Society for Testing and Materials, West Conshohocken, PA, 1999.
10. Powers, T. C., "A Discussion of Cement Hydration in Relation to the Curing of Concrete," *Proceedings of the Highway Res. Board*, 27, Washington, DC, 1947, pp.178~188.
11. Jeong, J. H., "Characterization of Slab Behavior and Related Material Properties Due to Temperature and Moisture Effects," *Ph.D. Dissertation*, Texas A&M University, College Station, TX, 2003.